Mat. Res. Soc. Symp. Proc. Vol. 674 © 2001 Materials Research Society

Epitaxial Growth of Dilute Magnetic Semiconductors: GaMnN and GaMnP

Mark E. Overberg, Cammy R. Abernathy, Stephen J. Pearton, Fred Sharifi [1], Arthur F. Hebard [1], Nineta Theodoropoulou [1], Stephan von Molnar [2], Madjid Anane [2], and Peng Xiong [2]
Department of Materials Science and Engineering, University of Florida, Gainesville, FL 32611, U.S.A.
[1]Department of Physics, University of Florida, Gainesville, FL 32611, U.S.A.
[2]Department of Physics and MARTECH, Florida State University, Tallahassee, FL 32306, U.S.A.

ABSTRACT

Epitaxial growth of the dilute magnetic semiconductors GaMnP and GaMnN has been investigated by Gas Source Molecular Beam Epitaxy (GSMBE). GaMnP films grown with < 4.5% Mn show the preferential formation of the second phases MnP and $Mn_{5.64}P_3$, resulting in only a slight deviation from purely diamagnetic behavior. GaMnN films grown on both Al_2O_3 and Metal-Organic Chemical Vapor Deposition (MOCVD) derived GaN surfaces show strong ferromagnetism when grown with either C codoping or at elevated temperatures to raise the concentration of n-type carriers. Comparable GaMnN films grown under conditions which produce highly resistive material show only paramagnetism, indicating the importance of carrier concentration on the resulting magnetic behavior. The formation of second phases was not observed in the GaMnN material for Mn concentrations less than 9%.

INTRODUCTION

Since the invention of the transistor, all facets of semiconductor electronics technology have been based upon the exploitation of the electron charge. Currently, a large research effort is centered upon methods to also exploit the property of electron spin. For many years it has been hypothesized that "spintronic" devices that utilize the quantum properties of the electron spin wavefunction will allow great advances in the development of electro-optic switches, ultra-sensitive magnetic field sensors, and particularly, quantum-based logic and memory for high speed computation[1-3]. However, its has been found that directly mating electronic materials (semiconductors) with spin materials (ferromagnetic metals) leads to interfacial problems due to the dissimilar nature of the materials' crystal structure, bonding, physical, and chemical properties[4]. Another solution is the dilute magnetic semiconductor (DMS), which consists of a semiconductor host heavily doped with a magnetic ion. A DMS material could permit direct integration with current semiconductor devices. Several theories have been presented on the nature of DMS-related ferromagnetism[5,6]. In the theory based upon a bound magnetic polaron (BMP) model, predicted Curie temperature (T_C) values are presented for 5% Mn in various III-V and II-VI semiconductors with a concentration of free holes equal to $3.5x10^{20}/cm^3$ [6]. To date, the best experimental T_C values for InMnAs, GaMnSb, and GaMnAs reasonably agree with theory, but are still well below room temperature[7-9]. The III-V DMS material GaMnN is predicted to have a T_C well above room temperature, while the material GaMnP is expected to be

more compatible with Si devices due to its close lattice matching. GaMnN has been produced in a powder form, but its application is limited[10]. In this paper, we demonstrate for the first time the thin film growth of the DMS materials GaMnP and GaMnN.

EXPERIMENTAL PROCEDURE

Films were grown by GSMBE in an INTEVAC Gas Source Gen II on In-mounted substrates. GaMnN films were grown on either (0001) Al_2O_3 substrates upon which a 20 nm low temperature AlN buffer layer (T_g = 435°C) was applied, or on MOCVD grown n-GaN layers on Al_2O_3 substrates. GaMnP films were grown on epi-ready (100) GaP substrates. The Al for the low temperature buffer layer was provided by a dimethylethylamine alane source. Shuttered effusion ovens charged with 7 N Ga and 4 N Mn provided the group III and the magnetic dopant fluxes. The C dopant was provided via a CBr_4 bubbler using 6 N He as the carrier gas, the CBr_4 being pyrolized at the substrate surface. GaMnP:C was grown with a CBr_4 flux sufficient to produce a hole concentration of $2.7x10^{20}/cm^3$ in GaP. The CBr_4 flux was held constant in all of the GaMnP growth runs. Reactive nitrogen for the GaMnN films was provided by an SVT RF plasma source operating at 375 W of forward power and a gas flow rate of 3 sccm N_2. Reactive phosphorous for the GaMnP films was provided by thermally cracked PH_3, at a flow rate of 1 sccm and a cracker temperature of 1050°C. X-ray diffraction (XRD) measurements were performed in a Philips APD 3720 powder diffractometer. Compositional information was provided by Auger Electron Spectroscopy (AES) in a Perkin-Elmer PHI 6600 system. Magnetic measurements were performed in a Quantum Design SQUID MPMS system. All Hall measurements were taken at room temperature in a custom built system using a 0.8 T electromagnet. Curie temperatures for ferromagnetic films were estimated by comparing the field cooled and zero field cooled curves at 500G.

RESULTS AND DISCUSSION

The Mn concentration in GaMnP was found to increase with increasing Mn cell temperature for Mn concentrations up to 8%. Growth temperature, T_g, was found to play a significant role in determining the number and type of phases found. At T_g = 600°C the Mn was found by XRD to incorporate as GaMnP and as MnP, which is orthorhombic. As T_g is reduced, the layers exhibit a mix of GaMnP, MnP and $Mn_{5.64}P_3$, which is hexagonal. For $T_g \leq 400$, $Mn_{5.64}P_3$ was found to be present in all of the films. In light of the multi-phase nature of these films it is not surprising that polycrystalline RHEED patterns were observed for all growth temperatures.

Electrically, Mn is expected to behave as a deep acceptor in GaP as it does in the case of GaMnAs. However, as the Mn concentration is increased, the hole concentration was found to decrease from the $2.7x10^{20}/cm^3$ in the GaP:C to $3x10^{18}/cm^3$ for an Mn concentration of 2.1%. Mn concentrations ≥ 4.2% produced semi-insulating films. It is possible that the reduction in hole concentration is due to the presence of the Mn_xP_y phases which are expected to be metallic. Magnetic measurements of the sample with 2.1% Mn and $p=3x10^{18}/cm^3$ showed a very slight deviation from pure diamagnetism in the M vs H data, as shown in Figure 1. Initial estimates suggest a T_C of ~50K. In light of the RHEED and XRD data it is likely that the magnetic behavior is due to the Mn_xP_y phases.

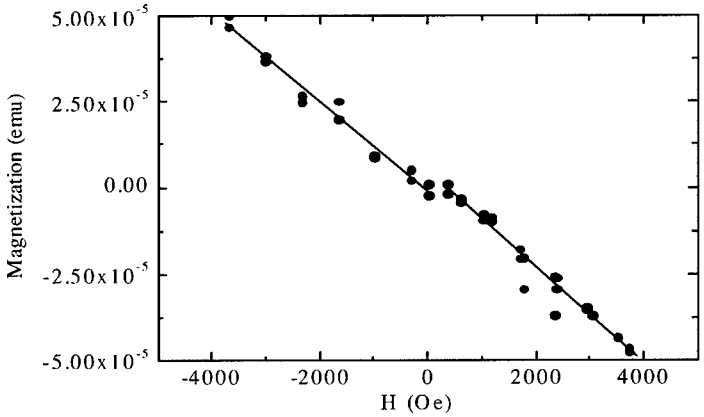

Figure 1. Magnetic characterization of GaMnP:C grown at 400°C. XRD indicates presence of MnP and $Mn_{5.64}P_3$ in addition to GaMnP:C.

Significantly better results were obtained with GaMnN. Because of the high vapor pressure of Mn, a lower growth temperature, 750°C, was used than is normally employed for growth of GaN in this system. Even this reduced temperature is significantly higher than is typically used for formation of III-Mn-V alloys. AES analysis showed the Mn incorporation to be linear with Mn cell temperature for Mn concentrations in the range of ~ 1.1% to 43.1%, as shown in Figure 2. The high concentrations that could be achieved suggest that in spite of the high vapor pressure, the Mn sticking coefficient is adequate even at elevated GaN growth temperatures. An XRD standard was grown using only Mn and the nitrogen plasma. The stable Mn_xN_y phase was found to be Mn_4N. However, when GaMnN films with concentrations less than 9% were examined, no evidence of this or any other Mn-containing phase could be found except for GaMnN. At very high Mn fluxes, additional MnGa phases were observed, suggesting that the metal flux exceeded the nitrogen flux in these films, resulting in the formation of metal rich phases. RHEED analysis showed evidence of 3D or polycrystalline structure. Increasing the growth temperature to 865°C improved the crystal quality, as evidenced by the appearance of a RHEED pattern that was a mixture of streaky and spotty patterns.

The GaN grown at T_g = 750°C was n-type with an electron concentration, n, of $n \cong 4x10^{19}/cm^3$. This large undoped background is believed to be due to a large concentration of nitrogen vacancies. As the Mn concentration was increased in the single-phase material, the GaMnN became increasingly resistive. This is in keeping with the expectation of a deep Mn acceptor that would serve to compensate the shallow nitrogen vacancy donor. At the very high Mn concentrations, Mn ≈ 47%, the films become conductive, presumably due to formation of the MnGa phases. It was found that the electron concentration could be increased either through the addition of carbon at the lower T_g, or by increasing the growth temperature. Using a CBr_4 flux previously calibrated to produce a carbon concentration of $\sim 10^{20}/cm^3$, an electron concentration in the GaMnN of $5 \times 10^{18}/cm^3$ was obtained. Under these growth conditions carbon typically produces highly resistive material. The fact that n-type GaMnN was observed suggests that the carbon is behaving as an amphoteric dopant in this material. Increasing the T_g to 865°C also

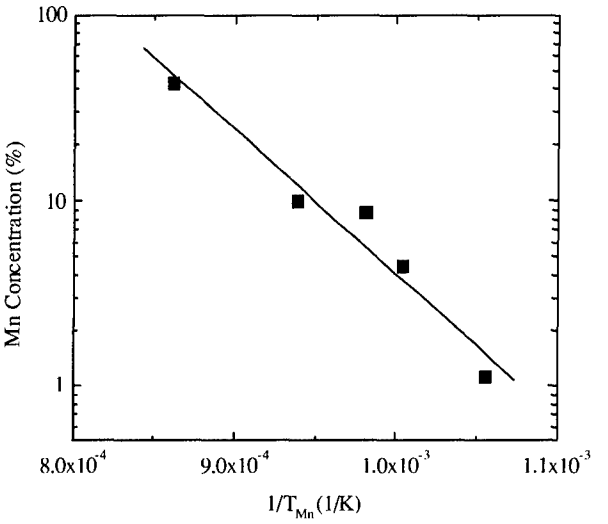

Figure 2. Variation of Mn concentration in GaMnN grown at 750°C as a function of reciprocal Mn cell temperature.

produced conductive GaMnN with $n \sim 1.5 \times 10^{19}/cm^3$. In this case the higher electron concentration is believed to be due to an increase in the nitrogen vacancy concentration caused by enhanced loss of nitrogen from the surface during growth at the higher temperature.

Magnetically, the higher carrier concentrations appear to be beneficial as the highly resistive films only show paramagnetic behavior. A rough estimate of these films shows a moment of 3.9 Bohr magnetons per Mn, suggesting that a significant fraction of the Mn ions are substitutional. In the conductive single-phase films, clear hysteresis was observed at 10 K, as shown in Figure 3, indicative of a ferromagnetic material. It was found that, at least for the lower T_g of 750°C, growing on an MOCVD buffer produced a higher saturation magnetization, $M_s \sim 2 \times 10^{-5}$ emu vs. 4×10^{-6} emu. This suggests that crystallinity plays a significant role in the magnetization since the MOCVD buffer is expected to produce superior growth. However, the T_c for both films was estimated to be ~ 100K, independent of the crystal quality. The more conductive material grown at 865°C showed similar behavior, though with a much higher saturation magnetization of 2×10^{-4} emu. The T_C was again estimated to be ~100K, and thus was not strongly affected by the change in carrier concentration. The appearance of ferromagnetism in samples both with and without C eliminates the formation of Mn-C complexes as the source of the ferromagnetic behavior in the samples grown at 750°C.

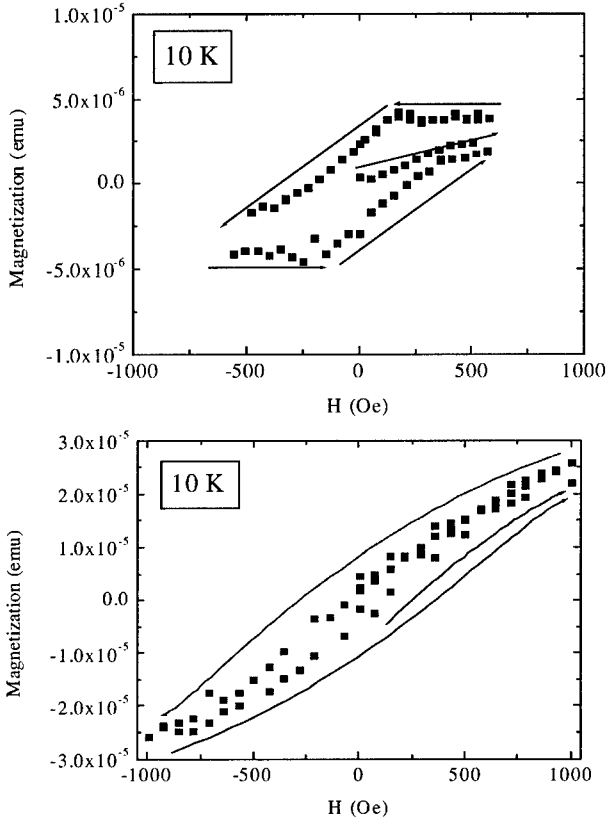

Figure 3. 10K magnetic characterization of GaMnN grown at 750°C on sapphire (top) or on an MOCVD buffer (bottom).

CONCLUSIONS

Synthesis of GaMnP and GaMnN by gas-source molecular beam epitaxy was investigated. For the case of GaMnP suppression of undesired Mn-containing phases was found to be extremely difficult. These second phases result in poor crystallinity as evidenced by RHEED and are most likely responsible for the slight deviation from pure diamagnetism observed in the M vs. H. data. GaMnN was found to be much more amenable to growth with single-phase material obtained for Mn concentrations up to 8%. The background electron concentration was found to drop as the Mn concentration was increased, resulting in semi-insulating material which showed only paramagnetic behavior when analyzed magnetically. Increasing the electron concentration either via the addition of carbon or by increasing the growth temperature produced ferromagnetic films with an estimated Curie temperature of ~100K. While improving the crystallinity and

increasing the electron concentration increased the saturation magnetization, they did not appear to strongly affect the Curie temperature. It is expected that increasing this parameter substantially will require the addition of Mg to produce a hole mediated Mn-Mn exchange interaction rather than an electron mediated Mn-Mn exchange interaction.

ACKNOWLEDGEMENTS

The authors would like to thank E. Lambers of the MAIC at the University of Florida for his assistance with the Auger Electron Spectroscopy analysis. Support for this work was provided by the U.S. Army Research Office under grant no. ARO- DAAG55-98-1-0216.

REFERENCES

(1) G. Prinz and K. Hathaway, Phys. Today **48**, 24-25 (1995).
(2) D. DiVencenzo, Science **270**, 255-261 (1995).
(3) D. Deutsch, Proc. R. Soc. Lond. A **400**, 97-117 (1985).
(4) M. Tanaka, J. Crys. Growth **201/202**, 660-669 (1999).
(5) B. Lee, T. Jungwirth, and A. H. MacDonald, Phys. Rev B **61** (23), 15606-15609 (2000).
(6) T. Dietl, H. Ohno, F. Matsukara, J. Cibert, and D. Ferrand, Science **287**, 1019-1022 (2000).
(7) H. Ohno, Science **281**, 951-956 (1998).
(8) H. Munekata, A. Zaslavsky, P. Fumagalli, and R. J. Gambino, Appl. Phys. Lett. **63** (21), 2929-2931 (1993).
(9) F. Matukura, E. Abe, and H. Ohno, J. Appl. Phys. **87** (9), 6442-6444 (2000).
(10) M. Zajac, R. Doradzinski, J. Gosk, J. Szczytko, M. Lefeld-Sosnowska, M. Kaminska, A. Twardowski, M. Palczewska, E. Grzanka, and W. Gebicki, Appl. Phys. Lett. **78** (9), 1276-1278 (2001).